Measurement and estimation of thermophysical properties of nickel based superalloys

P. N. Quested*[1], R. F. Brooks[1], L. Chapman[1], R. Morrell[1], Y. Youssef[2] and K. C. Mills[2]

Thermophysical properties for the solid and liquid phases of several Ni based superalloys (CMSX-4, CMSX-10, CM186LC, IN 738 and Rene 80) have been measured. The following properties were measured: heat capacity and enthalpy, thermal expansion coefficient and density, thermal diffusivity, viscosity and surface tension. Analysis of these measurements showed that that γ' phase (Ni_3Al) affected the values for the following properties; C_p, enthalpy, electrical resistivity, thermal diffusivity and conductivity. Relationships have been identified between properties and the γ' phase content (which can be represented by mass% Al in the alloy). These relations were then used to calculate property values of the alloys from chemical composition. Other relations were developed to estimate the viscosities and surface tensions of Ni based superalloys. The predicted property values were found to be in good agreement with the measured values.

Keywords: Nickel alloys, Surface tension, Viscosity, Thermal diffusivity, Latent heat, Specific heat, Modelling of properties

Dedicated to the memory of Professor Malcolm McLean

Introduction

This paper is dedicated to the memory of our former colleague Malcolm McLean who carried out so much classical work in identifying the problems associated with the solidification of nickel based superalloys and who was our treasured friend.

Mathematical modelling of the solidification process has proved to be an effective tool in overcoming problems and improving the quality of metal castings. They can identify those areas, which are prone to defects such as porosity or 'freckles'. It has been shown that the accuracy of model predictions improves with the use of more reliable data for the relevant thermophysical properties of the alloy.[1] Reliable data are needed for the properties affecting the fluid flow of the metal (density, viscosity and surface tension) and the heat transfer (heat capacity C_p, enthalpy, thermal diffusivity a and conductivity k).

Nickel based superalloys contain a number of different metallic elements. These can be divided into three types:

(i) nickel and other transition metals with similar properties (Co, Fe, Cr, Mn)

(ii) heavy, high melting metals such as W, Ta, Mo, Nb, Hf and Re, which provide high temperature solution hardening

(iii) elements such as Al and Ti, which improve mechanical strength by the formation of γ' phase precipitates. The first metal to solidify tends to be rich in the high melting elements; this leaves a liquid with a lower density. Subsequent convection can lead to the lighter liquid rising and knocking-off dendrite arms, which leads to the formation of misaligned grains.

There is a large number of commercial nickel based superalloys covering a wide range of compositions. Accurate values of the thermo physical properties are needed for this wide compositional range. The compositional ranges of interest are further widened when the compositions of solid and liquid formed during the solidification process are taken into account. Thus information is needed for the effect of chemical composition on the property values so that values can be calculated accurately for a wide range of alloy compositions. Thus, the objectives of this project were to provide accurate property values for a wide range of commercial alloys and to determine the effects of chemical composition on the property values in order to calculate property values for other alloy compositions.

Experimental

Ni based superalloys contain reactive metals (e.g. Al, Ti and Hf). These elements tend to react with the container material and with the gaseous atmosphere, thereby affecting the measured value. For this reason containerless methods are preferred especially for measurements on the liquid alloy. The National Physical Laboratory has developed a series of techniques to derive accurate

[1]National Physical Laboratory, Teddington, Middlesex, TW11 OLW, UK
[2]Department of Materials, Imperial College, London, SW7 2AZ, UK

*Corresponding author, email peter.quested@npl.co.uk

Published by Maney with permission of the National Physical Laboratory
Received 18 June 2008; accepted 17 July 2008
DOI 10.1179/174328408X361454

measurements of the thermophysical properties for both the solid and liquid alloys. Several of these methods use a levitated drop which eradicates reactions with the container.

Materials

The chemical compositions of the alloys used in this investigation are given in Table 1.

Experimental methods

The following techniques were used in the measurement of the thermophysical properties.

Density (ρ) and linear thermal expansion coefficient (α)

The density of the alloys at room temperature was measured by the Archimedean method. Density of the solid as a function of temperature was computed from the room temperature density and the linear thermal expansion coefficient (α) derived with a by a Linseis mechanical alumina dilatometer (by assuming α was isotropic). Density through the mushy region was determined using the technique of Piston dilatometry in which a small cylindrical sample is retained between ceramic pistons in a ceramic cylinder.[2] As melting proceeds the test sample expands and eventually collapses on melting. The cavity in the cell after collapse of the sample is filled thereby pushing the pistons outwards. The thermal expansion of the mush and liquid can be determined from knowledge of the thermal expansion of the cell material providing the cell does not leak.

Densities of liquid IN 718 alloy were determined using the levitated drop method[3,4] in which the levitated, molten drop of known mass in an Ar atmosphere is photographed in three directions, simultaneously. The sample temperature was determined by two colour pyrometry. The dimensions of the levitated drop were determined by comparing with the photographs of a drop of known dimensions.

Viscosity (η)

The viscosities of pure nickel and alloy IN 718 were measured using an Oscillation viscometer.[4,5] The viscosity was determined from the decay of the oscillations of a twisting sample. Specimens [24 (id) × 65 mm] were placed in a tight fitting alumina crucible. The crucible was suspended by a Pt–8%W wire (0·2 mm diameter) held in a thermostatted jacket at 30°C. The oscillations were followed by the movement of the reflected beam of laser light using a mirror mounted on the suspension wire. The reflected beam was detected by an array of light sensitive diodes placed in a circular arc. A waveform was deduced from the results from which the logarithmic decrement of the decaying sine wave could be determined. However, the Roscoe equation used to calculate the viscosity from the experimental results contains a typographical error. Consequently, the corrected version of this equation[6] was used to calculate the viscosities of the metal samples.

Surface tension (γ)

The surface tensions of the alloys were measured using the Levitated drop method.[4,7] The mass (m) of specimens (~0·5 g) was determined before and after the experiments. The measurements were carried out in an atmosphere of purified argon. The oscillation frequencies (ω_1, ω_2, etc.) of the drop were measured with a waveform analyser and temperatures were measured with a two colour pyrometer. Surface tensions were calculated from the Cumming's equation[8] using the Rayleigh frequency (ω_R) where z_0 is a gravitational element and r is the radius of the drop

$$\omega_R^2 = \sum \omega_1^2 + \omega_2^2 + \omega_3^2 + \omega_4^2 + \omega_5^2 \quad (1)$$

$$\gamma = (3/8)\pi m \omega_R^2 \quad (2)$$

Heat capacity (C_p), enthalpy ($H_T - H_{298}$) and enthalpies of transition and fusion (ΔH_{tr}, ΔH_{fus})

The heat capacity (C_p) and enthalpy of the various alloys were determined by differential scanning calorimetry (DSC). The C_p measurements for CMSX-4 and IN 718 were obtained between 298 and 1000 K using a Perkin Elmer DSC 7.[9,10] A stainless steel sample pan was heated (or cooled) at 10 K min^{-1} over the temperature range T_1 to T_2 for the following sequence with the sample pan

(i) empty
(ii) filled with a sapphire disc of known mass and heat capacity
(iii) filled with the alloy specimen.

The procedures used to derive the C_p have been reported elsewhere.[9,10]

The C_p measurements for temperatures between 1000 and 1750 K were obtained using a Stanton Redcroft DSC 1500.[11] A disc shaped sample was placed on an alumina disc sited in the bottom of a Pt crucible fitted

Table 1 Chemical compositions of alloys (mass%) and surface tension (γ^m) values at melting point for elements to be used in equation (11)

Alloy	%Ni	%Al	%C	%Co	%Cr	%Mo	%Nb	%Ta	%Ti	%W	Others
CMSX-4*	Bal.	5·6	0·006	9	6·5	0·6	–	6·5	1·0	6·4	Re 3 Hf 0·1
CMSX-10	Bal.	5·78	0·1	3·4	2·3	0·41		8·3	0·32	5·6	Re 6·4
CM186LC	Bal.	5·74	<0·05	9·4	6·0	0·5	–	3·5	0·74	8·5	Hf 1·32 Re 2·9
IN 718	52·5	0·5	0·08	1	19	3·1	5·2	–	0·9		Fe 16·7 Mn 0·35
IN 738	Bal.	3·53	0·1	8·26	15·85	1·73	0·82	1·73	3·49	2·57	
Rene 80	Bal.	2·95	0·17*	9·6	13·9	4·05	–	–	4·95	3·9	
γ^m, mN m^{-1}	1800	890		1900	1700	2250	1937	2050	1650	2320	Fe 1900 Re 2610 Zr 1500

Analysed composition unless indicated *Typical composition.

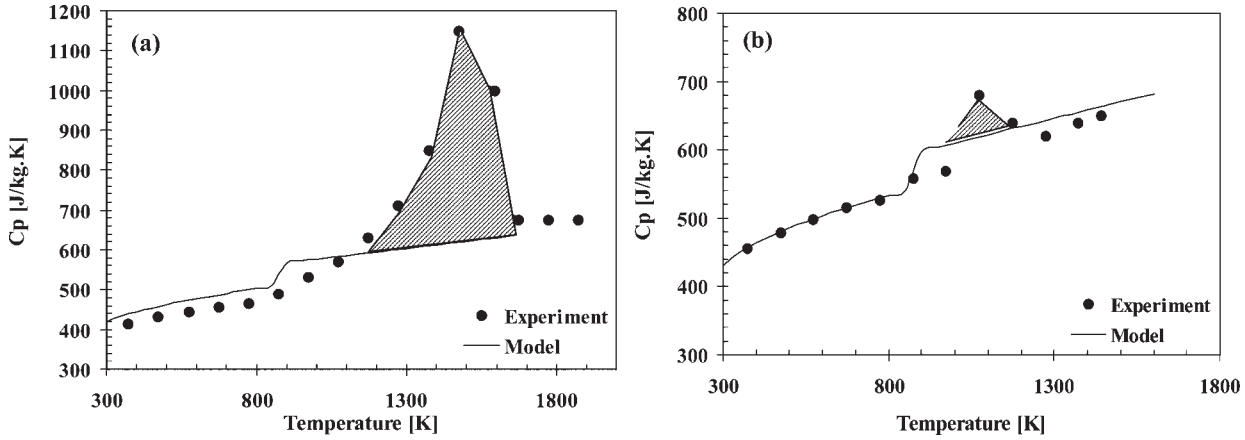

1 Heat capacity as function of temperature for *a* CMSX-4 and *b* IN718 showing method by which ΔH^{fus} was obtained[14]

with a Pt lid. A matched pan and lid was used as the reference. The procedures used to obtain the C_p and enthalpies were similar to those described above.

Enthalpies were derived by integrating the C_p–T relation between T_1 and T_2. Solidus (T^{sol}) and liquidus (T^{liq}) temperatures were obtained by applying the appropriate correction for 10 K min^{-1} for the onset temperature and the peak temperature respectively, associated with the fusion process. The corrections were established by measuring the onset and peak temperatures of calibrants (with known solidus and liquidus temperatures) at different heating rates and then extrapolating to zero heating rate.

Thermal diffusivity (a) and conductivity (k)

The thermal diffusivities of the alloys were measured using a Netzsch 427 Laser flash apparatus.[4,12] Disc shaped specimen 1–3 mm thick (L) were maintained in an atmosphere of purified argon. For measurements on solids the front face of the specimen was sprayed with graphite and a pulse of energy was focused on the front face and the temperature of the back face of the sample was monitored continuously with an InSb infra red detector.[4,12] For measurements of the liquid phase the sample was contained in a sapphire cell.

The thermal diffusivity of the sample at a specified temperature was determined from the temperature transient which yielded a value for the specimen to reach half of the maximum temperature rise ($t_{0\cdot5}$). The thermal diffusivity (a) was then determined from the following relation[13]

$$a = 0\cdot137L^2/t_{0\cdot5} \quad (3)$$

Thermal conductivity (k) values were calculated from the thermal diffusivity values and the relation, ($k = aC_p\rho$) and measured values of the C_p and density, except in the transition range where estimated C_p values were preferred.

Calculation of γ' fraction

The amount of γ' formed in the alloy was calculated using a thermodynamic software package.

Results and discussion

Measurements of the following properties (C_p, enthalpy, density, thermal expansion coefficient, thermal diffusivity) were carried out on the alloys, CMSX-10, CM186LC, IN 738 and Rene 80. Measurements of viscosity and surface tension were carried out on alloy IN 718.

The C_p–T curves for Ni based superalloys show evidence of several transitions which occur with increasing temperature:[14]

(i) around 870 K there is a step-like increase in the C_p ($\sim$50 J K^{-1} kg^{-1}) in all samples which has been attributed to the rearrangement of atoms
(ii) between 1070 and 1270 K the γ' phase coarsens which results in an increase in the C_p
(iii) between 1270 and 1500 K dissolution of the γ' phase (i.e. $\gamma' \rightarrow \gamma$) occurs and results in an increase in C_p culminating in a peak in the C_p–T curve
(iv) at temperatures >1550 K fusion of the sample occurs (mean T^{sol} and T^{liq} are 1600 ± 50 K and 1670 ± 50 K).

Transitions associated with both the coarsening and dissolution of the γ' phase (i.e. $\gamma' \rightarrow \gamma$) processes are both solid state transitions and are, consequently, somewhat sluggish. Both the C_p and thermal expansion measurements were carried out using dynamic techniques where the measurements are made at a set heating (or cooling) rate. The heating rates tend to be too fast for the C_p to come to an equilibrium value. So the recorded values are apparent (C_p^{app}) and not equilibrium (C_p^{eq}) values. Consequently, these apparent values are shown as dotted lines in the figures. Thus equilibrium values recorded in these transition ranges will be dependent upon both temperature and time. Thermal diffusivity measurements were made by heating to a specific temperature and allowing time for temperature equilibration before measurements were undertaken. Thus, the samples were much closer to equilibrium values than those obtained in the dynamic measurements. Electrical resistivity measurements in the transition ranges have been observed to change with time of annealing.[15]

The increases in C_p linked to the coarsening and the dissolution of the γ' phase suggested that these transitions are considered to be first order, i.e. they are associated with an enthalpy of transition (ΔH^{tr}) which is manifested by an apparent increase in C_p (in a similar way to values recorded for the fusion process, see Fig. 1). If the transitions are first order, estimated C_p values in the transition range should be used in calculating the thermal conductivity from thermal diffusivity measurements.

The measured values of the various properties obtained in this investigation are given in Table 2. These values are smoothed values taken from the curves. Measured values at temperatures in the transition ranges 1070–1470 K may not be true equilibrium values and could change with time.

Solidus (T^{sol}) and liquidus (T^{liq}) temperatures

The solidus and liquidus temperatures were obtained from the DSC and piston dilatometry results. For DSC experiments, the values of T^{sol} and T^{liq} were derived from the onset and peak temperatures recorded on the heating cycle after correcting for the heating rate (10 K min^{-1}). The results obtained from the two studies are given in Table 3.

It can be seen from the table that the recorded values for T^{sol} and T^{liq} are not in very good agreement. The differences in these values originate from differences in the measurement techniques. In DSC the measurements are carried out at a heating rate of 10 K min^{-1} and the solid needs time to react to a transition (including fusion). Consequently, measured T^{sol} and T^{liq} tend to be higher than the true transition temperature and the correction term, $\Delta T=(T^{meas}-T^{actual})$ tends to increase with increasing heating rate.

In piston dilatometry, when the sample begins to melt, the increase in volume is, at first accommodated in the gaps between the sample and the cell. The piston only responds when (i) all the gaps are filled or (ii) the sample collapses completely. This point is denoted the softening point and occurs above the solidus temperature. Softening temperatures will only approximate to the solidus temperature when the sample collapses near T^{sol}.

Heat capacity and enthalpy

The C_p results obtained for alloys CMSX-4 and -10, CM186LC, IN 718 and 738 and Rene 80 are shown in Figs. 1–3. It can be seen from the results for CMSX-4

Table 2 Experimental data for thermophysical properties of alloys. (2) Estimated C_p, (H_T–$H298$) for Rene 80 and IN 738

Alloy	T^{sol}–T^{liq}, K	Properties	298 K	400 K	600 K	800 K	1000 K	1200 K	1400 K	T^{sol}	T^{liq}	1700K
CMSX-4		C_p, J K^{-1} kg^{-1}	397	419	448	471	540*	650*	925*		630	630
	1593–1653	H_T–H_{298}, kJ kg^{-1}	0	42	129	222	325	443				
		Density ρ, kg m^{-3}	8700	8652	8559	8466	8374	8283	8193	8107	7754	7710
		Thermal expansion coefficient α, $\times 10^6$ K^{-1}										
		Thermal diffusivity a, $\times 10^6$ m^2 s^{-1}		2·5	3·1	3·8	4·35	4·7	5·1		4·9	4·9
		Thermal conductivity k, W m^{-1} K^{-1}		9·0	12·0	15·4	19·9	21·9	24·4			25
CMSX-10		C_p, J K^{-1} kg^{-1}	395†	418†	446†	468†	536†	645*	805*	880*	630	630
	1635–1683	H_T–H_{298}, kJ kg^{-1}	0	42	128	220	324	324	554		948†	965
		Density ρ, kg m^{-3}	9046	9014	8945	8872	8793	8705	8600	8442	8133	8128
		Thermal expansion coefficient α, $\times 10^6$ K^{-1}	–	11·5	12·5	13·1	13·7	14·5	15·7			
		Thermal diffusivity a, $\times 10^6$ m^2 s^{-1}	2·43	2·73	3·30	3·88	4·47				5·1–6·2	
		Thermal conductivity k, W m^{-1} K^{-1}	8·7	10·3	13·2	15·5	21·1					
CM186		C_p, J K^{-1} kg^{-1}	395†	418†	446†	468†	538†	630*	680*	1100*	720	720
	1540–1666	H_T–H_{298}, kJ kg^{-1}	0	42†	128†	220†	327†	445†	568†		955	1003†
		Density ρ, kg m^{-3}	8689	8661	8595	8523	8445	8355	8238	~8200	8147	
		Thermal expansion coefficient α, $\times 10^6$ K^{-1}	–	10·6	12·2	13·0	13·7	14·8	16·6			
		Thermal diffusivity a, $\times 10^6$ m^2 s^{-1}	2·23	2·54	3·12	3·71	4·30	4·50	4·75			
		Thermal conductivity k, W m^{-1} K^{-1}	7·7	9·2	12·0	14·8	19·5	23·7	26·6			
IN738		C_p, J K^{-1} kg^{-1}	450†	473	511†	547†	631†	675*	8925*		700	700
	1512–1628	H_T–H_{298}, kJ kg^{-1}	0	47†	146†	251†	371†	500	637			
		Density ρ, kg m^{-3}	8177	8148	8082	8012	7934	7840	7702	7600	7324	7280†
		Thermal expansion coefficient α, $\times 10^6$ K^{-1}	–	11·8	13·1	13·8	14·6	15·9	18·7			
		Thermal diffusivity a, $\times 10^6$ m^2 s^{-1}	2·65	2·96	3·53	4·10	4·67	4·70	4·87			
		Thermal conductivity k, W m^{-1} K^{-1}	9·8	11·4	14·6	18·0	23·4	24·9				
Rene 80		C_p, J K^{-1} kg^{-1}	457†	480†	519†	557†	644†	681†	1100*	750	830	830
	1485–1611	H_T–H_{298}, kJ kg^{-1}	0	48†	148†	255†	377†	509†	649			
		Density ρ, kg m^{-3}	8130	8101	8037	7966	7891	7798	7666	7600	7359	7300
		Thermal expansion coefficient α, $\times 10^6$ K^{-1}	–	11·6	12·8	13·6	14·4	15·7	18·5			
		Thermal diffusivity a, $\times 10^6$ m^2 s^{-1}	2·77	3·04	3·56	4·08	4·60	4·93			4·46	
		Thermal conductivity k, W m^{-1} K^{-1}	10·3	11·8	14·8	18·1	23·4	26·2				

*Measured value in transition range.
†Calculated using adopted procedures.
†Extrapolated.

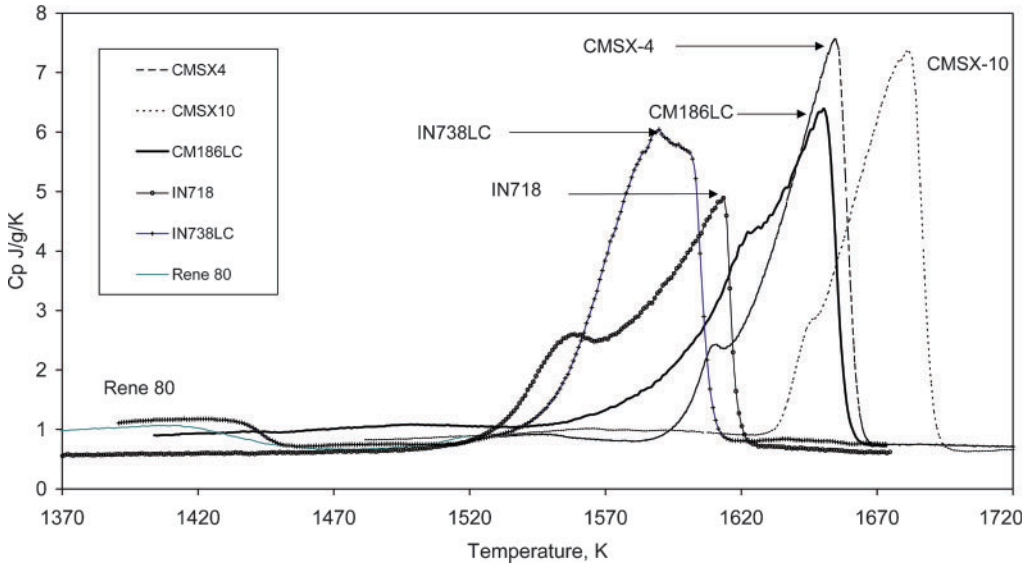

2 Typical measured C_p–temperature curve for selected Ni based superalloys

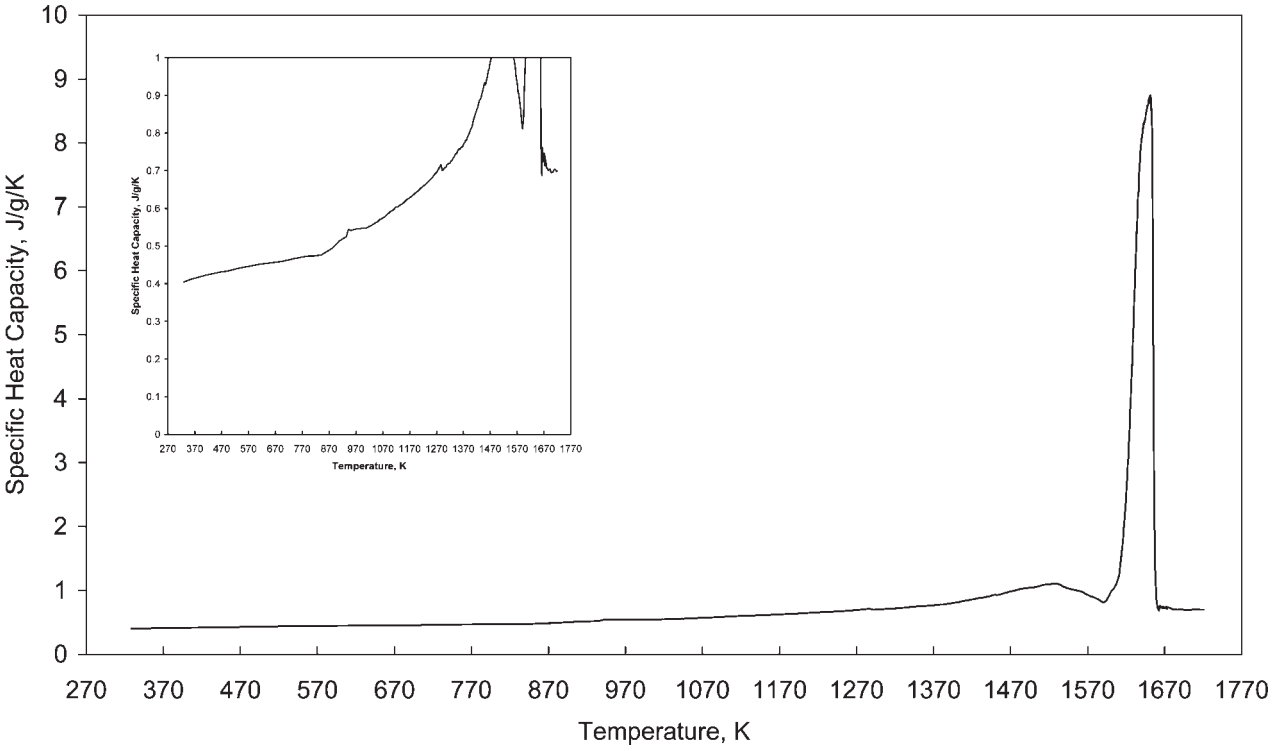

3 Heat capacity as function of temperature for CMSX-4 showing typical transitions

that anomalies in the C_p–T curve (due to transitions) occur in the region 1200–1300 K

Inspection of the results obtained here and in other investigations indicated[14] that:

(i) measured values for enthalpy of fusion ΔH^{fus} for all alloys had a value of $\sim 225 \pm 25$ kJ kg^{-1}

(ii) experimental C_p values for the liquid phase of different alloys showed considerable scatter.

Table 3 Comparison of melting range values obtained with DSC and dilatometry and recorded values for enthalpy of fusion

	CMSX-4		CMSX-10		CM186LC		IN738		Rene 80	
	T^{sol}, K	T^{liq}, K	T^{sol}, K	T^{liq}, K	T^{sol}, K	T^{liq}, K	T^{sol}, K	T^{liq}, K	T^{sol}, K	T^{liq}, K
DSC	1593	1653	1635	1683	1540	1666	1512	1628	1485	1611
Dilatometer			1625	1701	1578	1618	1573		1605	1598
ΔH^{fus}, kJ kg^{-1}	240*		207*	222†	232*	190†	282*	255†	209*	250†

*,†denote values for heating and cooling curves respectively.

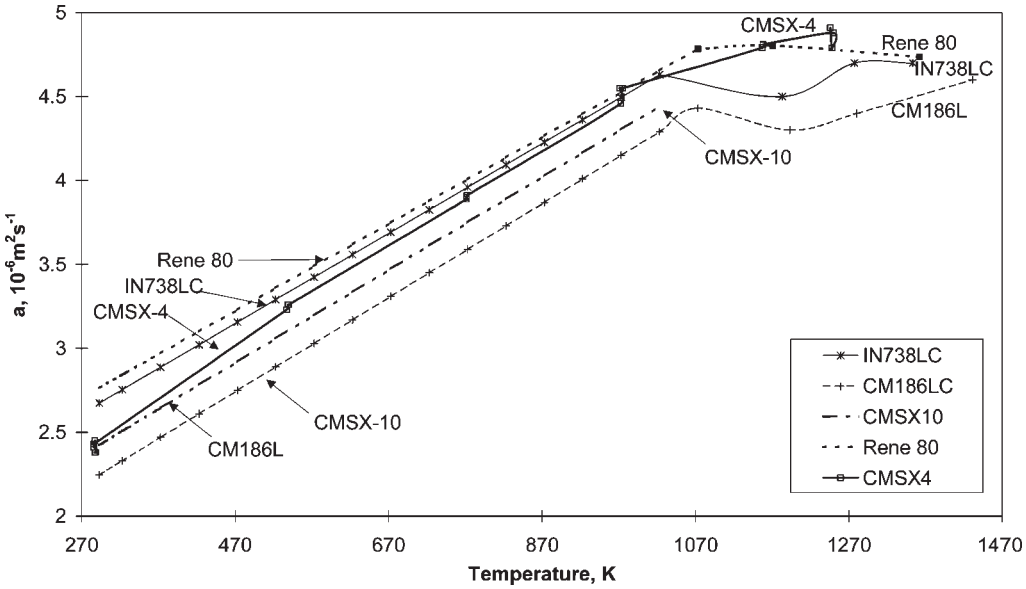

4 Thermal diffusivity as function of temperature for alloys, IN738LC, Cm186LC, CMSX-10, Rene 80 and CMSX-4

Thermal diffusivity (a) and conductivity (k)

Thermal diffusivity values for alloys CMSX-4 and -10, CM186LC, IN738 and Rene 80 are plotted in Fig. 4. Thermal diffusivity, conductivity and electrical resistivity are all dependent upon electron transport. Consequently, for the solid phase measured values are affected by the microstructure since electrons can be scattered by particles, grain boundaries, etc. Thus, there tends to be some variation in thermal diffusivity values for the solid phase since they are dependent upon the microstructure which is, in turn, dependent on the thermal history of the specimen. Measured thermal diffusivity values derived in the temperature ranges where the γ' phase particles coarsen and then dissolve also tend to vary because these transformations are dependent upon both temperature and time. It was also found that:

(1) values recorded for different liquid phase alloys varied between 4 and $6{\cdot}8 \times 10^{-6}$ m^2 s^{-1} (mean value of $a_{(l)}$ for the liquid phase $= 5{\cdot}1 \times 10^{-6}$ m^2 s^{-1})

(2) values recorded for the 'mushy' range tend to be unreliable since some of the heat supplied is not conducted but used to melt the alloy.

Thermal conductivity values were calculated from thermal diffusivity, density and Cp values are given in Table 2. Estimated C_p values in the transition range were used in these calculations since the measured C_p values in the transition range (1070–1470 K) are apparent C_p values (i.e. they contain enthalpy contributions).

Density (ρ) and thermal expansion coefficient (α)

Density and thermal expansion values obtained with piston dilatometer for the alloys CMSX-4 and -10, CM186LC, IN 738 and Rene 80 are given in Figs. 5 and 6 respectively. Values for CMSX-4 in the liquid phase were also obtained using the levitated drop method.[3,4]

Viscosity (η) measurements

Viscosity measurements were obtained by oscillation viscometry for alloy IN718 and for pure nickel as shown in Fig. 7. It can be seen that values for IN 718 are in excellent agreement with those reported by Overfelt *et al.*[16] The temperature dependence of the viscosity for alloy IN 718 can be expressed by the following equation

$$\eta\,(\text{m Pa s}) = 0{\cdot}196\exp\,(5848/T) \qquad (4)$$

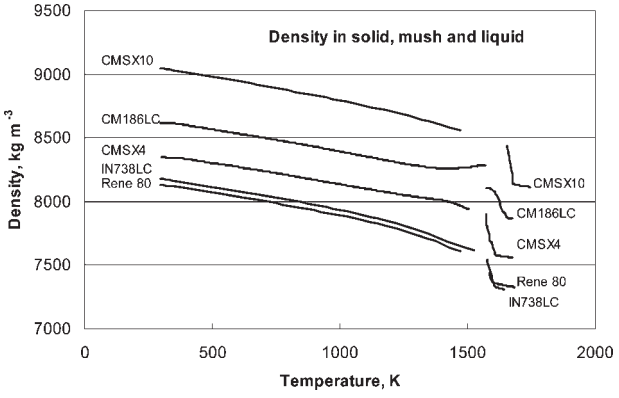

5 Density as function of temperature for alloys CMSX-10, CMSX-4, CM186LC, IN738LC and Rene 80

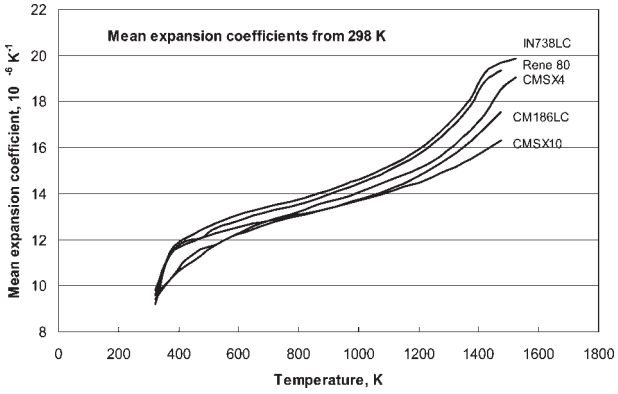

6 Mean thermal expansion coefficient as function of temperature for alloys CMSX-10, CMSX-4, CM186LC, IN 738 and Rene 80

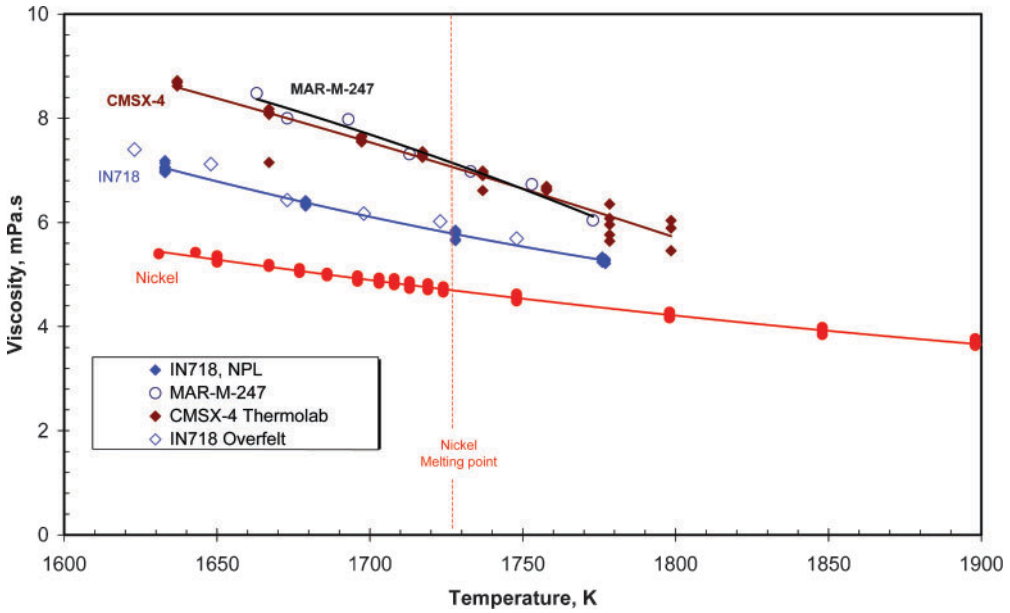

7 Viscosity of alloy IN 718, CMSX-4, MAR-M-247 and pure Ni as function of temperature; open symbols IN 718 and MAR-M-247 due to Overfelt *et al.*[16]

Surface tension (γ) measurements

The surface tension values of alloy IN 718, obtained with the levitated drop method are shown in Fig. 8.[4,17] Surface tension (γ) and its temperature dependency ($d\gamma/dT$) are both very sensitive to the levels of soluble oxygen and sulphur. The sample studied had a sulphur content of 10 ppm. Values were only obtained for temperatures $\sim$1850 to $\sim$2100 K;[4,17] the temperature dependence for the surface tension is given by the following equation

$$\gamma(\text{mN m}^{-1}) = 1842 - 0{\cdot}11(T - 2000\ \text{K}) \quad (5)$$

Effect of γ' phase on properties

As mentioned above, the γ' phase precipitates formed in the γ phase matrix provide high temperature strength by hindering the movement of dislocations. The principal constituent of the γ' phase is Ni_3Al but Ni_3Fe and Ni_3Cr also contribute but dissolve in the γ matrix at 793 and 823 K respectively. Consequently, these compounds do not contribute to the γ' phase above 823 K. The γ' phase content was calculated using thermodynamic software.

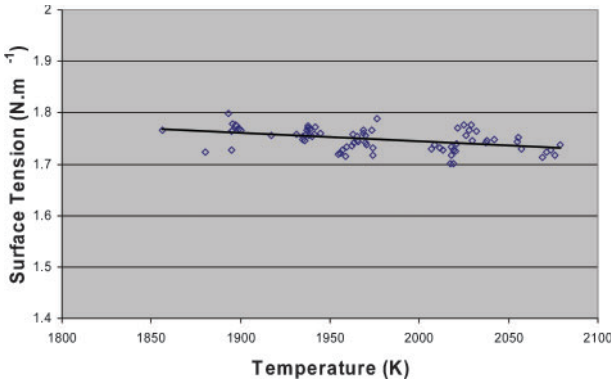

8 Surface tension of alloy IN718 as function of temperature[17]

Since Ni_3Al is the principal constituent of the γ' phase the amount of γ' phase was expressed as a function of the Al content of the alloy. The following relation was found[13,18]

$$\gamma'(\text{at.}-\%) = 16{\cdot}1 + 10{\cdot}6(\text{wt}-\%\text{Al}) \quad (6)$$

Inspection of the results showed that the properties (P) such as the density may be affected by the amount of γ' phase present in the alloy. Consequently, the difference in property (ΔP) between the measured (P^{meas}) and ideal (P^{ideal}) property values ($\Delta P = P^{meas} - P^{ideal}$) was determined by using equation (7) where X is the mole fraction and i refers to the various elements in the alloy

$$P^{ideal} = \sum X_i P_i \quad (7)$$

The differences in properties, ΔP_T (C_p, density, thermal conductivity k and diffusivity a and electrical resistivity) at any specific temperature were then plotted as functions of the γ' phase content (usually represented by mass% Al).[13,18] Typical results are shown in Fig. 9. It can be seen that:

(i) ΔP_T is a linear function of the Al content (Figs. 9 and 10)

(ii) ΔP_T values for the liquid phase are also linearly dependent upon the Al content, showing that the properties even in the liquid are affected by the strong bonding between the Ni and Al atoms

(iii) the enthalpy of transition (ΔH^{tr}) associated with the coarsening and dissolution of the γ' phase particles was calculated by integrating $\Delta C_{p\,T}$ for the temperature range of the transitions (shaded region in Fig. 1); ΔH^{tr} was also found to be a linear function of the Al content (Fig. 10*b*)

(iv) the temperature dependency of the property (P–T curve) was also affected by the Al content (Fig. 11)

(v) no relation was established between the viscosity, surface tension and the enthalpy of fusion (ΔH^{fus}) with γ' phase (or Al) contents.

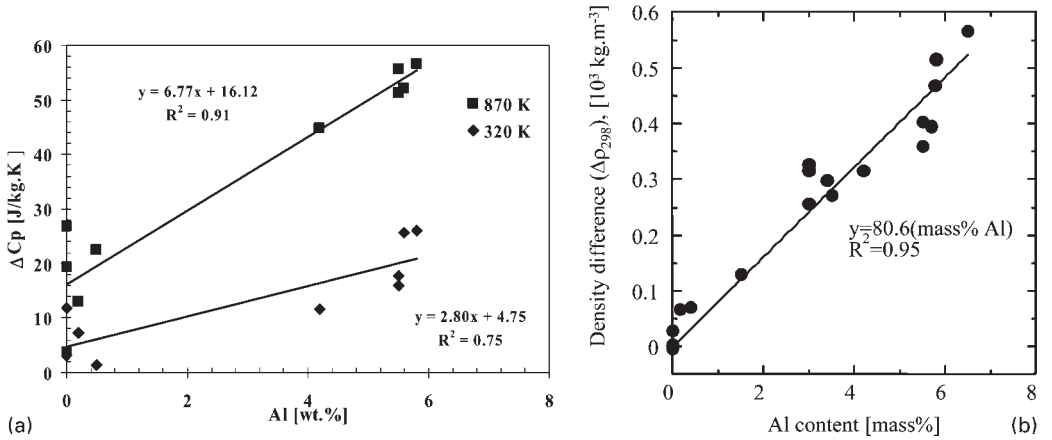

9 Differences in *a* heat capacity at 320 and 870 K and *b* density at 298 K of Ni based alloys as function of Al content

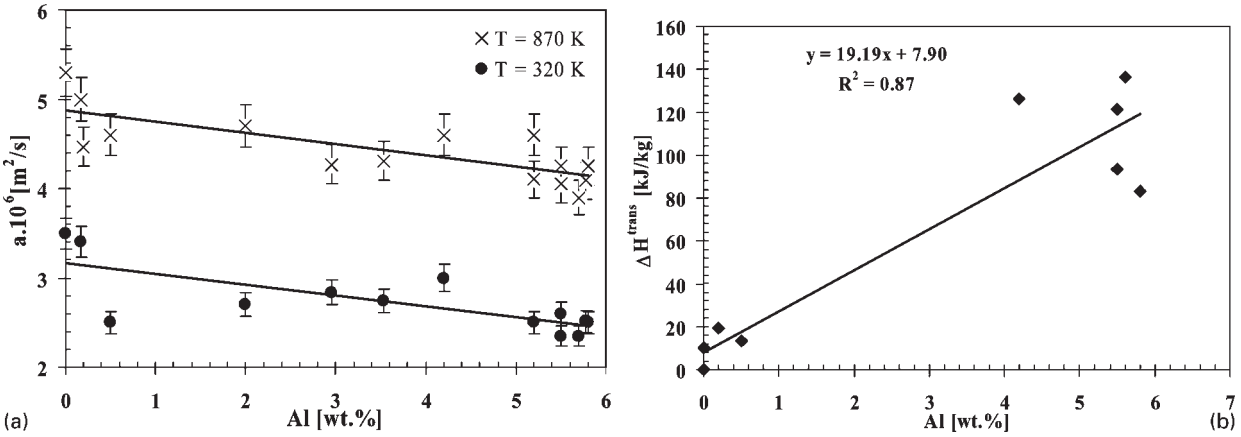

10 *a* thermal diffusivity and *b* enthalpies of transition for combined coarsening and $\gamma' \rightarrow \gamma$ transformations as functions of Al content

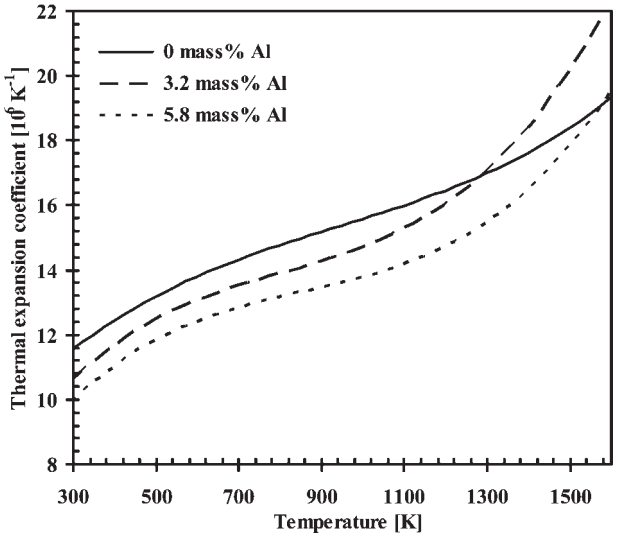

11 Thermal expansion coefficient as function of temperature for superalloys with different Al contents

Estimation of properties

It was mentioned above that it is necessary to derive property–temperature relations for a wide range of alloy compositions. Consequently, relations derived above in the section on 'Effect of γ' phase on properties' have been developed to enable property–temperature relations to be calculated from chemical composition for the alloys. Other routines have been developed for the estimation of viscosity and surface tension.

Properties estimated from relation with Al content

The C_p, enthalpies (H_T–H_{298}) density, thermal diffusivity (a) and conductivity (k) and the electrical resistivity were calculated[19] from

(i) ΔP_T–Al% relations established (e.g. Figs. 9 and 10)

(ii) the temperature dependency as a function of Al content of the alloy (Fig. 11).

The calculated values were in good agreement with measured values, values of the parameter $[100(P^{meas}–P^{calc})/P^{meas}]$ were typically C_p and enthalpy ($\pm$2–5%), density ($\pm$2%), thermal diffusivity and conductivity ($\pm$5%) electrical resistivity ($\pm$10%).

Solidus (T^{sol}) and liquidus (T^{liq}) temperatures

Numerical analysis of literature data for solidus (T^{sol}) and liquidus (T^{liq}) temperatures yielded[19] the following relations

$$T^{liq}(K) = 956.9 + 8.2\,Y_{Ni} + 7.6\,Y_{Co} + 2.2\,Y_{Al} + 3.4\,Y_{Ti} - 3.7\,Y_{Ta} + 3.9\,Y_{Cr} + 7.2\,Y_{Mo} + 11.5\,Y_{W} + 21.1\,Y_{Re} + 12.1\,Y_{Ru} + 7.4\,Y_{Fe} - 3.3(Y_{Nb} + Y_{Hf}),\ R^2 = 0.94 \quad (8)$$

$$T^{sol}(K) = -120 + 17.7\,Y_{Ni} + 16.0\,Y_{Co} + 15.2\,Y_{Al} + 2.1\,Y_{Ti} - 13.4\,Y_{Ta} + 19.2\,Y_{Cr} + 5.0\,Y_{Mo} + 20.4\,Y_{W} + 34.3\,Y_{Re} + 23.1\,Y_{Ru} + 15.4\,Y_{Fe} - 6.4(Y_{Nb} + Y_{Hf}),\ R^2 = 0.83 \quad (9)$$

where $Y_i = 100X_i$

Most calculated values for T^{sol} and T^{liq} lie within ± 10 and ± 5 K respectively.

Viscosity

The viscosities of liquid Ni based superalloys can be estimated[19] using the following equation developed during this investigation

$$\log_{10}\eta^{alloy}(\text{m Pa s}) = 2570/T - 0.8224 + 1.75\times10^{-3}\,Y_{Cr} + 1.1\,Y_{Fe} + 10.2\times10^{-3}\,Y_{heavy} \quad (10)$$

where Y_i=mass% of element i and Y_{heavy}=total mass% of heavy elements (i.e. Σ%W+%Re+%Hf+%Nb +%Ta+%Mo).

The calculated values were in good agreement with measured values.

Surface tension (γ)

The principal factor affecting the surface tension (γ) and ($d\gamma/dT$) is the soluble oxygen (O%) content. The surface tension of the alloy is calculated in the following manner:

(i) the surface tension of the alloy (γ^{m}_{alloy}) with zero O and S concentration was calculated at the mean T^{liq} value of 1650 K using equation (11) and the values of γ^{m} given in Table 1

$$\gamma^{m}_{alloy} = \sum X_i\gamma^{m}_{i} \quad (11)$$

(ii) the temperature dependence was assumed to be $-0{\cdot}4$ mN m^{-1} K^{-1} identical to that of pure Ni

$$\gamma_{alloy,T}(\text{mN m}^{-1}) = \gamma^{m}_{alloy} - 0{\cdot}4(T - 1650\text{K}) \quad (12)$$

(iii) the effect of O and S can be calculated using equations (13) to (17) based on the analogous Fe–O and Fe–S systems[20] and where the equilibrium absorption coefficients are given by $\gamma_O = 2{\cdot}0\times10^{-8}$ and $\gamma_S = 1{\cdot}4\times10^{-8}$ mol m^{-2}

$$\ln K_o = -1{\cdot}85 + (13200/8{\cdot}314T) \quad (13)$$

$$\ln K_S = -5{\cdot}75 + (20000/8{\cdot}314T) \quad (14)$$

$$F = 8.314T\Gamma_O\{1 + K_o(\text{mass\%O}) + K_S(\text{mass\%S})/[1 + K_S(\text{mass\%O})\} \quad (15)$$

$$G = 8.314T\Gamma_S\{1 + K_O(\text{mass\%O}) + K_S(\text{mass\%S})/[1 + K_O(\text{mass\%O})\} \quad (16)$$

$$\gamma_{sup\ alloy} = \gamma_{alloy} - F - G \quad (17)$$

Calculated values were usually within ± 5% of measured values.

Conclusions

1. The γ' phase content of the alloy has a significant effect on the following properties and their temperature dependencies: C_p, enthalpy, density, thermal diffusivity and conductivity and electrical resistivity.
2. The γ' phase content can be calculated from the amount of Al (wt-%).
3. The property values for the liquid were affected by the aluminium content of the alloy showing the strong bonding of Ni and Al atoms persists into the liquid phase.
4. The strong negative departures from Raoult's law result in higher surface tension values than those calculated for an ideal system.
5. The experimental scatter associated with the measurement of C_p, thermal diffusivity and electrical resistivity of liquid alloys is currently too large to determine the effect of Al content on these properties; more accurate measurements are required
6. Reliable values for the thermophysical properties of other Ni based superalloys can be estimated from chemical composition using methods developed in this project.

Acknowledgements

The work at Imperial College was funded by EPSRC Grant No. GR/S45768/01. The help provided by Dr Zushu Li, and Dr Yuchu Su (both formerly Imperial College) is gratefully acknowledged.

The NPL work was funded by DIUS (formerly DTI) as part of the Materials Measurement Programme.

References

1. S. Oxley, P. N. Quested and K. C. Mills: Proc. AVS Conf., 49; 1999, American Vacuum Society, Santa Fe, New Mexico.
2. R. Morrell and P. N. Quested: *High Temp. High Pres.*, 2003, **35–36**, 417–435.
3. R. F. Brooks, B. Monaghan, A. J. Barnicoat, A. McCabe, K. C. Mills and P. N. Quested: *Int. J. Thermophys.*, 1996, **17**, 1151–1161.
4. K. C. Mills: 'Recommended values of thermophysical properties for selected commercial alloys'; 2002, Abington, Publ. Woodhead.
5. R. F. Brooks, A. P. Day, R. J. L. Andon, L. A. Chapman, K. C. Mills and P. N. Quested: *High Temp. High Pres.*, 2001, **33**, 72–82.
6. D. Ferriss and P. N. Quested: 'Some comparisons of the Roscoe and Beckwith-Newell analyses for the determination of viscosity of liquid metals using the oscillating cup viscometer', NPL report CMMT (A), 306, 2000.
7. K. C. Mills and R. F. Brooks: *Mater. Sci. Eng. A*, 1994, **A178**, 77–81.
8. D. Cummings and D. Blackburn: *J. Fluid Mech.*, 1991, **224**, 395.
9. M. J. Richardson: 'Compendium of thermophysical measurement techniques', (ed. K. G. Maglic, A. Cezairliyan and V. E. Peletsky), Vol. 2; 1992, New York, Plenum Press.
10. K. C. Mills and M. J. Richardson: *Thermochim. Acta*, 1937, **6**, 427–438.
11. L. A. Chapman: *J. Mater. Sci.*, 2004, **39**, (24), 7229–7236.
12. B. J. Monaghan and P. N. Quested: *ISIJ Int.*, 2001, **41**, 154.
13. C. D. Henning and R. Parker: *J. Heat Transfer*, 1967, **39**, 146.
14. K. C. Mills, Y. Youssef and Z. Li: *ISIJ Int.*, 2006, **46**, 50–57.
15. G. I. Rosen, S. F. Dirnfeld, M. Bamberger and B. Prinz: *Z. Metallkd.*, 1994, **85**, 127.
16. R. A. Overfelt, C. A. Matlock and M. E. Wells: *Metall. Trans. B*, 1996, **27**, 698.
17. R. F. Brooks, B. Monaghan, A. J. Barnicoat, A. McCabe, K. C. Mills and P. N. Quested: *Int. J. Thermophys.*, 1996, **17**, 1151.
18. Z. Li and K. C. Mills: *Met Mater. Trans. B*, 2006, **37B**, 781–790.
19. K. C. Mills, Y. Youssef, Z. Li and Y. Su: *ISIJ Int.*, 2006, **46**, 623–632.
20. Y. Su, K. C. Mills and A. Dinsdale: *J Mater. Sci.*, 2005, **40**, 2185.